

## HGCDTE APDS FOR TIME RESOLVED SPACE APPLICATIONS

J. Rothman<sup>1</sup>, G. Lasfargues<sup>1</sup>, B. Delacourt<sup>1</sup>, A. Dumas<sup>2</sup>, F. Gibert<sup>2</sup>, A. Bardoux<sup>3</sup>, M. Boutillier<sup>3</sup>  
<sup>1</sup>CEA/Leti, France, <sup>2</sup>LMD-IPSL, France, <sup>3</sup>CNES, France

### I. INTRODUCTION

HgCdTe APDs have opened a new horizon in photon starved applications due to their exceptional performance in terms of high linear gain, low excess noise and high quantum efficiency. Both focal plane arrays (FPAs) and large array single element using HgCdTe (MCT) APDs have been developed at CEA/Leti and Sofradir and high performance devices are at present available to detect without deterioration the spatial and/or temporal information in photon fluxes with a low number of photon in each spatio-temporal bin. The enhancement in performance that can be achieved with MCT has subsequently been demonstrated in a wide scope of applications such as astronomical observations, active imaging, deep space telecommunications, atmospheric LIDAR and mid-IR (MIR) time resolved photoluminescence measurements. Most of these applications can be used in space borne platforms.

In the present communication we will focus on our recent development and tests of detectors for applications that only require the temporal information and can be addressed using single element MCT APDs, such as LIDAR and high data rate free-space optical communication. The use of MCT APD for these applications will be discussed in section II in perspective of how the gain, dark current and response time varies as a function of Cd composition and operating temperature. The discussion will be illustrated, in section III, by the performance obtained detector assemblies using large area high operating temperature (190 K) APDs, in which we typically obtain noise equivalent powers in the range of 25-80 fW/ $\sqrt{\text{Hz}}$  for bandwidth ranging from 20 to 200 MHz. In particular, we report results obtained on an APD detector that has been used by Laboratoire de Meteorologie Dynamique (LMD) to perform DIAL-LIDAR measurements at 2  $\mu\text{m}$  up to distance close to 10 km and discuss the performances that can be achieved using MCT APDs in free space optical telecommunications up to 10 Gbit/s data rates and/or at single photon detection limit.

The results of first space reliability tests made on Leti HgCdTe APDs, in collaboration with CNES are presented in section IV. The space reliability test consisted of proton irradiation and endurance at  $T=-85^\circ\text{C}$  operation and with variable reverse bias. The conclusion and perspective for the use of HgCdTe APDs for space applications are finally presented in section V.

### II. HgCdTe APDs FOR TIME RESOLVED APPLICATIONS

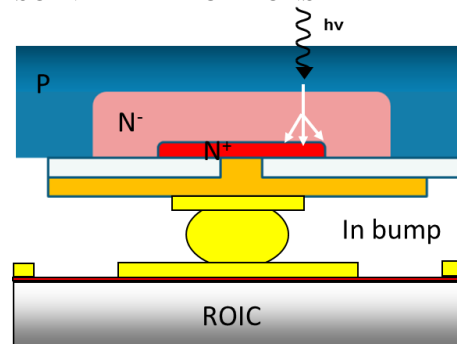


**Fig. 1.** Illustration of a backside illuminated planar HgCdTe APD made at CEA/Leti.

The MCT APDs made at Leti and Sofradir are manufactured using liquid phase epitaxial grown epi-layers with close to constant Cd composition. A homo-junction with a large n- region is formed by an n-type conversion of a spatially localized region close to the device surface. The schematic illustration of the structure is shown in Fig. 1. The thickness of the P layer is adapted to ensure a full absorption of the photons. The created minority electrons diffuse to the depleted n- region where the avalanche gain multiplication takes place. The thickness and the pixel pitch define the diffusion volume that is responsible for the dark current at high operating temperature. At low operating temperature the dark current is mainly generated in the depleted multiplication region, through trap and tunnelling mechanisms that are enhanced by the electric field. The P-type doped absorption layer in Fig. 1 is directly exposed to the incoming photon flux when the substrate used to grow the absorption layer has been removed. Such substrate removal is a standard process for detectors manufactured at CEA/Leti with a cut-off wavelength longer than 2.5  $\mu\text{m}$  and enable an efficient and constant collection of photons, corresponding to a quantum efficiency above 90 %, from the ultra-violet range 280 nm up to the IR cut-off wavelength. This panchromatic behaviour was first reported for a 5.5  $\mu\text{m}$  cut of MCT APD [1] and extends the potential use of

theses detectors to the visible and ultraviolet spectral range when a low number of photons needs to be collected during a short observation.

HgCdTe e-APDs with high gain and low dark-current have been developed with cut-off wavelengths ( $\lambda_c$ ) ranging from 2.5 to 5.6  $\mu\text{m}$  by adjusting the Cd composition in the absorption and multiplication regions. Gain curves measured at  $T=80$  K for APDs with various  $\lambda_c$  are compared in Fig 2. The close to constant exponential increase of the gain observed for all composition is directly related to the exclusive avalanche multiplication of electrons which is responsible for the low excess noise in MCT APDs. It can be seen that the gain at constant reverse bias decreases with  $\lambda_c$ . The variation in gain is mainly due to the increase of the bandgap. The APDs with the highest  $\lambda_c=8.8$   $\mu\text{m}$  display exponential gain but are not directly useful at low fluxes due to increased tunnel currents associated with the smaller band gap. With the present state of the art of the MCT APDs technology at CEA, MWIR and SWIR cut-off APDs can be used for low flux and/or fast observation down to uv wavelengths.

The exact value of the excess noise factor  $F$  can only be estimated from observations of probability density function (PDF) of APD gain in detectors with single photon resolution. This level of sensitivity have been demonstrated by DRS and CEA/Leti achieved using MCT APDs hybridised onto a high bandwidth and low noise CMOS amplifier [2,3]. This demonstration has enabled direct estimations of the gain PDF at CEA/Leti using a buffered source follower pre-amplifier with a bandwidth of 10 MHz and rms noise of 15 electrons. This detector assembly enables single photon detection at APD gains of about 50 and gain PDF and  $F$  estimations at gains higher than 100 [3]. Figure 3 reports the estimation of the gain PDF in a MCT APD with a cut-off wavelength of  $\lambda_c=3.66$   $\mu\text{m}$ , measured at 80 K with an average gain close to 100. The distribution corresponds to an excess noise factor of  $F=1.23$ , well within the range of the values typically found in the literature  $F=1.1-1.4$ . The variations of the reported excess noise factors is due to contributions from the geometry of the APDs to the excess factor and from errors in the estimation of  $F$ , due to variations of the collection efficiency of the APD before avalanche multiplications [4]. Associated with the typically high quantum efficiency in MCT photodiodes, the QE to  $F$  (QEFR) ratios are typically higher than 50 % for all  $\lambda_c$ . QEFR measures the conservation of the information contained in a shot noise limited photon flux in linear amplified photo-detectors and the values observed in MCT APDs are the highest achieved in any solid state linear detector.

The response time of MCT APDs is fundamental for the range of applications that can be addressed with theses detectors. It is dependent on three contributions: a) the collection time of primary photo generated electrons, b) the multiplication region transit time of carriers generated during the avalanche process and c) the RC constant of the diode. The collection time can be minimised by using thin absorption layer, concentrating the light absorption in the middle of the junction and by forcing a drift collection through the presence of a doping and/or bandgap gradient. The exclusive electron multiplication in MCT APDs is a major advantages, as it implies that only one transit time needs to be accounted for each type of carriers. Hence, the gain do not directly influence the transit time why ultra-high gain bandwidth products can be achieved in theses detectors [5,6,7]. The highest measured bandwidth of 800 MHz for  $M=100$  is thought to be limited by impedance miss-match in the inter-connexion circuit used to enable a backside illumination of the diode [7]. The average transit velocities of the electrons and the holes have been estimated from variation of the shape of the response time. These values shows that bandwidth in excess of 10 GHz are achievable in MCT APDs and the application requirements for such detectors are further discussed in section III B.

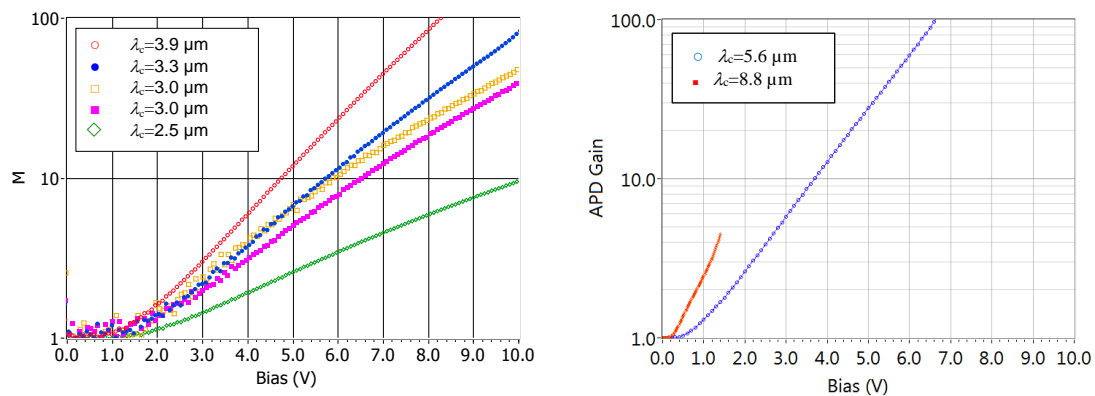
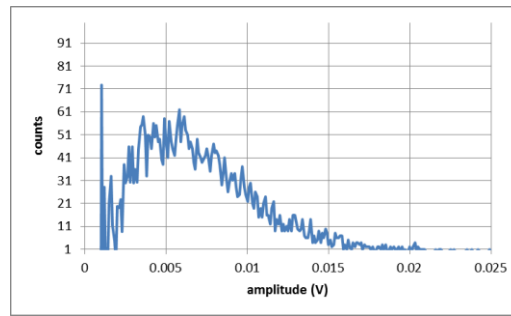
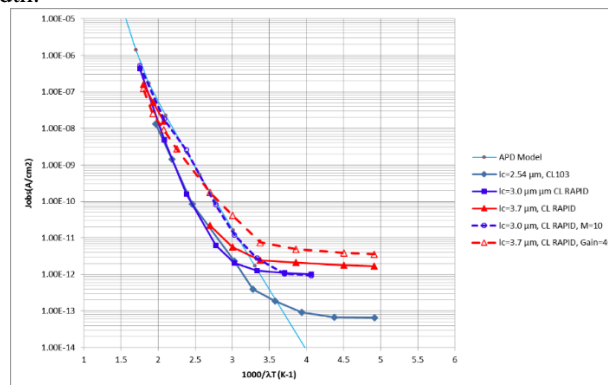


Fig. 2. MCT APD gain measured at  $T=80$  K for APDs with cut off wavelengths ranging from 2.5 to 8.8  $\mu\text{m}$ .



**Fig. 3.** Estimation of the APD gain PDF from asynchronous detection of thermal single photons and by subtracting ROIC noise and dark current events. The corresponding excess noise factor is equal to  $F=1.23$

The sensitivity of a photodetector is ultimately limited by the fluctuations in dark current. The dark current in MCT APDs have been measured as a function of temperature using arrays of APD hybridised on low noise read out integrated circuits (ROICs). Figure 4 reports gain normalised dark currents measured in MCT APD with and without gain as a function of cut-off wavelength normalised inverse temperature,  $1/T\lambda_c$  [8]. It can be seen that the dark current with and without gain have a similar dependence on  $1/T\lambda_c$ . At high temperature (low  $1/T\lambda_c$ ) the APD are limited by a diffusion current and the gain normalised dark current is similar with and without gain. At lower temperature, the dark current with gain is approximately 10 times higher than the current without gain. This shows on an enhanced thermal emission in the junction, correlated with the increased applied field that can be translated as a reduced Shockley-Read-Hall (SRH) life-time in the multiplication layer. At lower temperature, the apparent dark current is limited by the glow of the read-out circuit. The level of the glow varies between 1 and 200 electrons per second, due to difference in ROIC design and configuration during the measurements. The experimental data is compared to values calculated with a phenomenological model that been developed that describes the variation of the dark current as a function of  $x_{Cd}$ . A good description of the experimental data is observed for  $\lambda_c=2.5-4 \mu\text{m}$ . A slightly higher dark current can be expected for higher gains. In the following section, this model will be used to predict the performance of MCT APDs with different composition and coupled to preamplifier with different levels of noise and bandwidth.



**Fig. 4.** Gain normalised dark current compared to modelled dark current as a function of the  $\lambda_c$  normalised inverse temperature for APDs with an without gain and with  $\lambda_c$  varying from 2.5 to 3.6  $\mu\text{m}$

### III. HgCdTe APDS DETECTORS FOR TIME RESOLVED APPLICATIONS

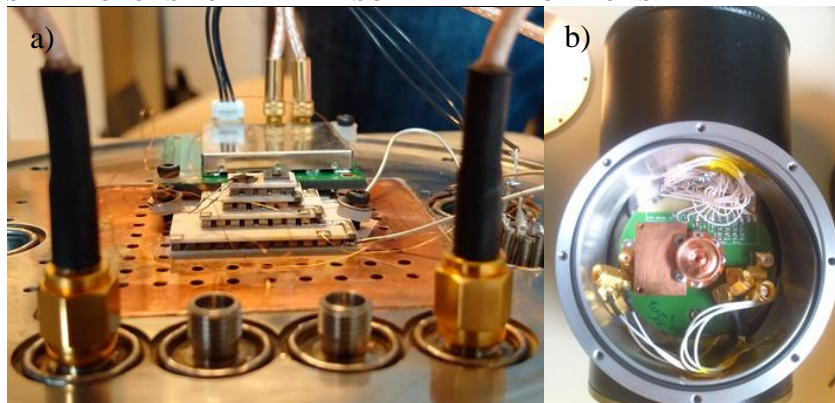


**Fig. 5.** Images of a) the high temperature TEC cooled detector module and b) the LN2 cryostat.

Two generic detector packages have been developed so far. The first one, pictured in figure 5 a), was developed for application requiring high operating temperatures between 180 and 300K, uses 4-stage Peltier module (or TEC) to control the temperature of the APD. By definition, this configuration is most adequate for high bandwidth applications in which a small amount of dark current during the observation time. If the lower range of operating temperature is needed for such applications, it is preferable to deport the pre-amplifier beside the TEC stage to avoid additional thermal dissipation. This type of detector was used during the LOCL demonstration using MCT APDs in 2014 and for first direct detection DIAL lidar measurement of CO<sub>2</sub> using APDs. The characteristics of the detector module used for this experiment is detailed in sub-section A. MCT APDs module with optimized bandwidth in excess of 1 GHz can be used with a similar package for free space optical communication and the expected performance of such detectors is presented in sub-section B.

In application requiring higher sensitivity, we are currently integrating the detector and pre-amplifier in LN2 deware. Figure 5 b) illustrates such a detector module in which a PCB is used to support the APD-CMOS hybrid and amplify the output signal and two copper cold screens are used to screen out thermal photons on and from the APD and the amplifier, respectively. This approach is currently considered for making the next generation of fast signal element detectors for lidar and telecom application with resolutions in the single photon range. The expected performance and required operating temperature of MCT APD detectors for single photon resolved free space telecom are further discussed in subsection B.

#### A. HgCdTe APD for atmospheric LIDAR

A first detector module for LIDAR applications have been delivered to Laboratoire de Météorologie Dynamique (LMD) and integrated in the COWI set-up [9]. Figure 6 illustrates the detector module mounted at the output of a 200 mm telescope which collects the backscattered light from the pulses emitted by the lasers on and off the CO<sub>2</sub> absorption peak. The detector module includes a 20 MHz trans-impedance amplifier (TIA) and the measured output noise is 1.65 pA/√Hz at unity gain over BW=14.5 MHz. The noise level is slightly higher than nominal amplifier noise, most probably due to a large additional capacitance in the inter-connection circuit used to form the backside illuminated 200 μm APD detector. An operating temperature of 185 K is achieved using the 4 stage TEC element illustrated in Fig 5. After alignment of all optical elements in figure 6, a coupling efficiency of a collimated input light was estimated to be close to be 54 % (81 % when corrected from the expected transmission of the optical elements in the set-up). The corrected value is close to the measured unity gain quantum efficiency of 72 %. The expected gain and equivalent noise with a BW of 14.5 MHz is illustrated in figure 7. At the nominal reverse bias of 12 V that has been used at LMD, the equivalent input noise is about 80 photons rms. At higher reverse bias, the detector noise starts to be limited by the detected background IR flux to about 25 photons rms at 16 V, which corresponds to a NEP of 25 fW/√Hz. A higher sensitivity can be achieved by reducing the amplifier noise and the IR background to values below 10 fW/√Hz (less than 10 photons) at constant operating temperature. Lower operating temperatures will be needed to achieve higher sensitivities, approaching single photon resolution.

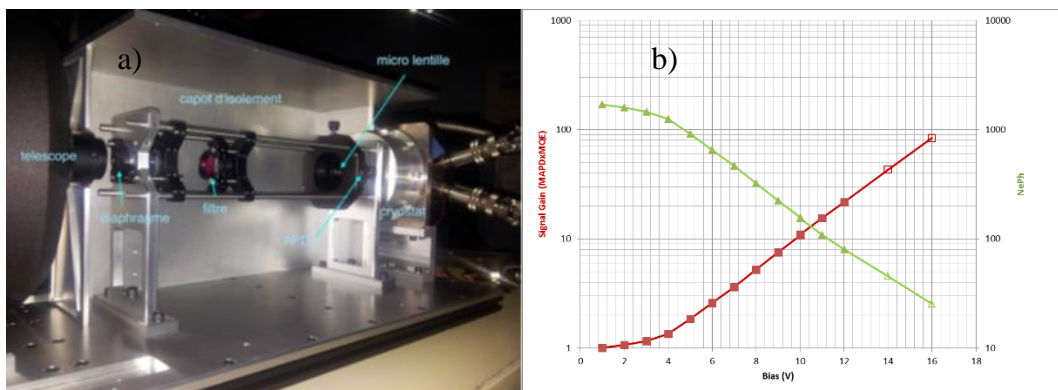


**Fig. 6.** a) Integration of the MCT APD detector module in the COWI LIDAR set-up and b) measured APD gain and sensitivity of 200 μm MCT APDs detector modules operated at 190 K with a bandwidth of 14.5 MHz

First atmospheric direct detection DIAL measurements have been performed using the MCT at LMD since the end of 2015. Figure 7 reports a typical signal recorded for the laser off wavelength with the samples averaged over 9 s. An aerosol signal is observed up to a distance of 20 km. The signal to noise (SNR) ratio is high enough to estimate the absorption from CO<sub>2</sub> have been estimated with a precision ranging from 1 to 10 % for signals that have been averaged over an observation time of 4 s and estimated over a distance of 100 to 3000 m. It should be strained that the average signal is quite low and that the SNR for most of the sampled points is limited by the noise from the TIA and not by the photon shot noise. Hence, a higher APD gain  $M$  would enable to reduce the acquisition time by a factor  $M^2$ . Another limitation is related to the observation of a long time settling signal

characterized by an exponential decay that interferes with the LIDAR signal when the on wavelength is placed close to the center of the absorption peak. This parasitic signal seems to be at least partially induced by the APD and further investigation will be made to study and to reduce the impact of this phenomena that can be limiting in the most demanding LIDAR applications.

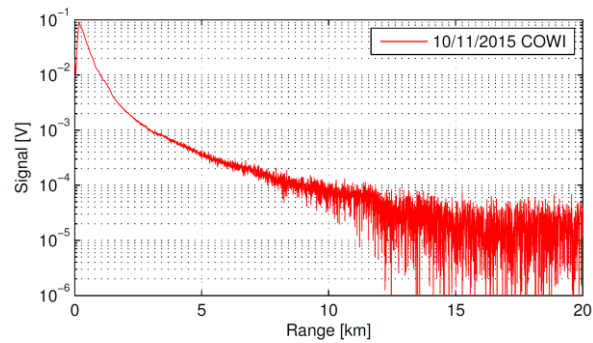


**Fig. 7.** Return signal collected with MCT APD in the COWI set-up with an. The return signal from a distance corresponds to about 1 photons per 25 ns (BW=20 MHz)

*B. HgCdTe APDs for free space optical communications*

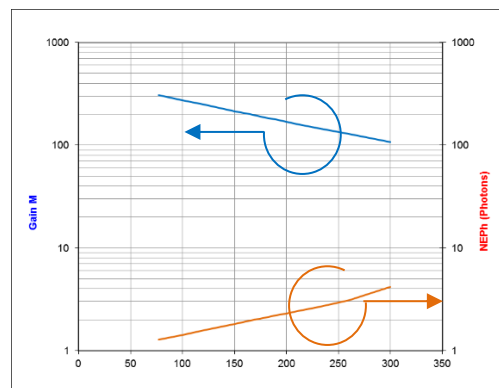


**Fig. 8.** Modelled APD gain and sensitivity (NEPh) of 15  $\mu\text{m}$  with  $\lambda_c=2.8 \mu\text{m}$  HgCdTe APD operated at fixed bias (17.5 V) and coupled with a 10 GHz bandwidth TIA with an equivalent input current noise density of 10  $\text{pA}/\sqrt{\text{Hz}}$ .

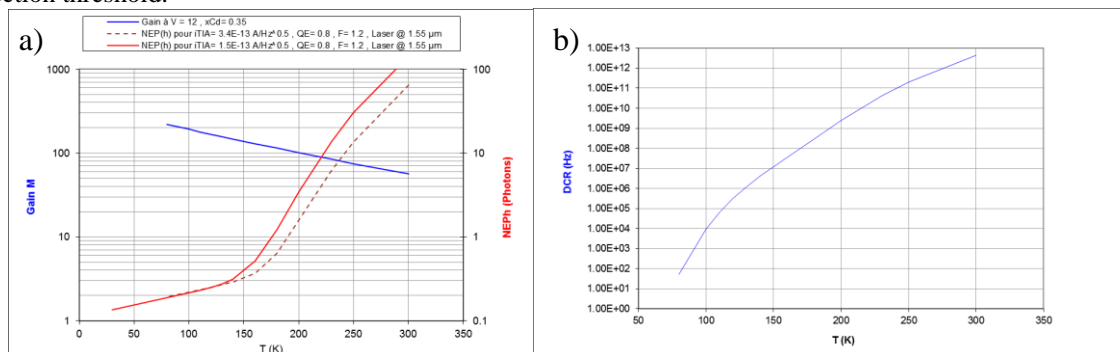
Free space optical communication have attracted an increasing attention over the last years, fueled by successful demonstrations of high data rate links between satellites [10] and from satellites to earth over very large distances[11,12]. Consequently, FSO is currently considered both for high data rate satellite network for global coverage and to increase the amount of data that can be transmitted during mission into deep space. MTC APDs are particularly promising for these applications as they can be used at high bandwidth and gain with free space coupling, which allows to reduce their size and consequently increasing the operating temperature at constant sensitivity.

Figure 8 shows an example of the expected performance of MCT APDs with an optimized bandwidth of 10 GHz. At this level of gain, in the order of 100, the sensitivity is limited by the amplifier noise up to  $T=250 \text{ K}$ . A small contribution from the dark current is observed at 300 K, which limits the sensitivity to a value around 5 photons rms. This example shows that MCT APDs with high bandwidth can be used with close to photon counting resolution up to ambient temperature if the light can be concentrated on small enough surface. It is strained that this is simplified compared to fibre optical amplifiers as the APD is free space coupled with high angular acceptance which allows to minimize the spot size without degrading the coupling efficiency. Larger diodes can also be used

For deep space optical communication, the number of photons that can be detected are strongly reduced and the achievable data rates are limited both by the bandwidth accessible for very high sensitivity detectors, requiring down to single photon resolution, and the increased laser output power needed to squeeze in the same number of photons into a shorter time slot. A bandwidth between 200 MHz and 1 GHz is expected to be sufficient for most applications. To achieve single photon resolution it is important to minimize the noise of the preamplifier to a value below 100 electrons rms and it is preferable to hybridize the APD directly on the amplifier. Hence, the amplifier must be operated at lower temperature and the choice in technology is at present limited to the once that

have been validated at low temperature and is compatible with hybridization. At LETI we are currently working on the design of fast amplifier with a minimal bandwidth of 200 MHz.

The sensitivity for MCT APD coupled to preamplifier with a noise of 33 electrons rms over a bandwidth of 200 MHz and 1 GHz is reported as a function of operating temperature in figure 9 a). At low operating temperature, the noise is limited by the amplifier and both detectors perform equally at a single photon detection level. At higher temperatures, the dark current gives a dominating contribution to noise and set a limit to the photon-counting regime at around 140 to 150 K for the 200 MHz and 1GHz module, respectively. The difference in sensitivity is directly related to the difference in BW as more dark event will be integrated during the characteristic time of the lower bandwidth detector. The actual operating temperature once the photon counting limit has been achieved depends on the dark count rate that can be acceptable in each application. Figure 9 b) shows an estimated level of DCR for an APD with the same geometry and composition as in figure 9 a). For example, a detector module with a bandwidth of 200 MHz requires an operating temperature of less than 120 K to reach a DCR of 200 kHz, corresponding to an error probability of about 0.1 % per observation time. The actual error rate at this temperature might be lower as the dark current events at low temperature are generated in the multiplication layer and do not experience a full amplification and can, in consequence, be discharged by a properly adjusted event detection threshold.



**Fig. 9.** a) Modelled sensitivity of MCT APD detectors with a diameter of 30  $\mu\text{m}$  and  $\lambda_c=3.6 \mu\text{m}$  coupled to low noise pre-amplifiers with a noise of 33 electrons rms over 0.2 and 1 GHz and b) associated DCR.

#### IV. SPACE RELIABILITY TESTS ON CEA/LETI HgCdTe APDS

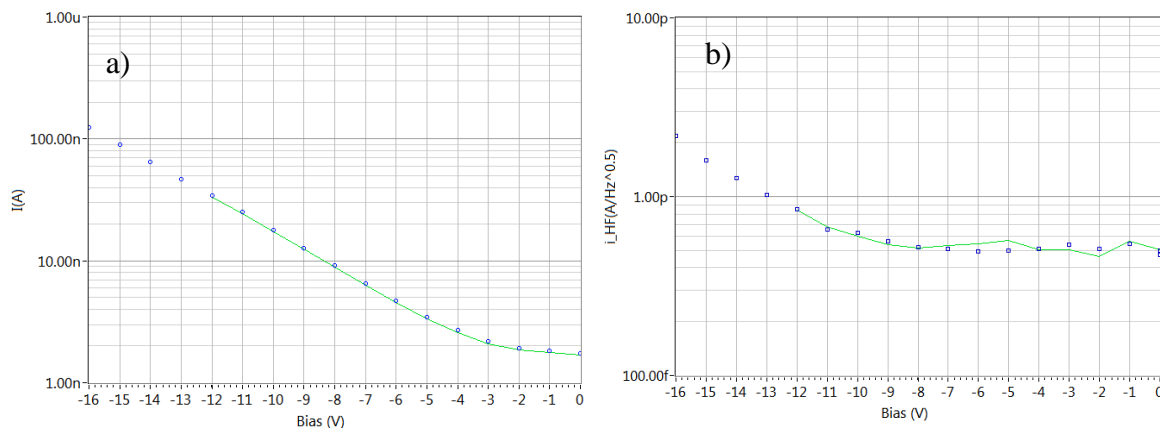


**Fig. 10.** Variation of a) output current and b) average current noise spectral density as a function of reverse bias before (continuous line) and after (squares) proton irradiation.

First space reliability tests have been performed on CEA/Leti's MCT APDs in collaboration with CNES. The goal was not only to test the resistance of the devices to protons irradiation, but also to test how the devices supports to be operated under longer periods at high reverse bias and operating temperature using a combined step stress and endurance approach. A 200  $\mu\text{m}$  diameter APD with  $\lambda_c=2.8 \mu\text{m}$ , identical to the one integrated in the lidar prototype, was operated at  $T=-85^\circ\text{C}$  and at a reverse bias 12 V while irradiated with 180 MeV protons up to a fluence of  $10^{11} \text{ cm}^{-2}$ . The combined step-stress and endurance tests were made by sequentially operating the APD at reverse biases of 12, 14 and 16 V for 1000 h at each bias. The endurance test was performed both on the irradiated and a non-irradiated APD. The APD current was measured using an external trans-impedance amplifier with a bandwidth of 60 kHz and a gain of 1 MV/A. The responsivity was measured during the test by turning on and of a CW fiber laser

Figure 10 a) and b) illustrates the variation of the background current and the current noise spectral density at 9.3 kHz on the irradiated APD before and after irradiation and the full endurance test. The unity gain current level and the noise at high reverse bias is limited by the thermal flux on the detector. The performance in terms of gain and high frequency noise of the detector is found to be constant for this level of stress of the APDs. This observation was confirmed by the observation of an equally constant performance during the endurance test of the non-irradiated APD.

The low frequency noise and the quantum efficiency was however found to be impacted by the irradiations. The variation of responsivity and quantum efficiency are reported in table 1. A reduction of the response (and QE supposing constant gain) is observed after irradiation. This reduction indicates the generation of defects that reduces the collection of carrier in the quasi neutral absorption layer and/or reduces the gain. The reduction seems to have been at least partially suppressed after the first 1000 h of operation at 12 V. This indicates that the defects are partially cured or passivated with time. If this is confirmed, the responsivity of the detector should not be impacted by the low flux of protons in space as the responsivity of the detector will have the time to recover between the radiations events. The protons did also introduces an increase of 1/f noise of a factor 2, as illustrated in figure 11. The associated defects do not appear to be cured during the operation of the APD, although a slight decrease in the 1/f is observed after 1000 h operating at 12 V. The influence of the 1/f noise and its small increase depends strongly on the application and system characteristics, such as the laser repetition rate for DIAL measurements which should ideally be higher than 1/f frequency corner, observed around 300 Hz in figure 13.

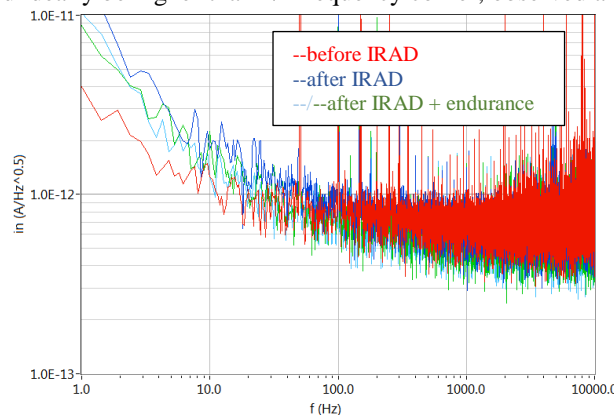


Fig. 11. Current noise spectral density before and after irradiation and endurance at a reverse bias of 12 V.

Tab. 1. Laser response of the 200  $\mu\text{m}$  MCT APD detector before and after irradiation.

Mesurement	$V_{\text{APD}}$ (V)	$P_{\text{opt}}$ (W)	$I_{\text{light}}$ (A)	QE
Before IRAD	1.0	1.15E-08	1.06E-08	0.74
Before IRAD	12.0	5.25E-09	4.73E-09	0.72
After IRAD	12.0	5.25E-09	4.07E-09	0.62
After endurance	12.0	5.25E-09	4.56E-09	0.69

#### IV. CONCLUSION AND PERSPECTIVES

The use of MCT APDs for time resolved single element applications with sensitivity down to a single photons has been discussed in perspectives of MCT APDs characteristics, recently developed demonstrator results and estimated performances for future high sensitivity high bandwidth applications such as FSO communications. An MCT APD detector module with a sensitivity down to 25 fW/ $\sqrt{\text{Hz}}$  has been used to perform first DIAL lidar detection of CO<sub>2</sub> in the direct mode using a solid state detector. The sensitivity in the first demonstrations was mainly limited by the TIA noise to precisions levels of about 1 to 10 %. Some systematic errors was however observed. For example, a long term settling time was found to limit the capacity to estimate the CO<sub>2</sub> concentration in some experimental configurations. The long term settling time have been partially attributed to the APD and further studies is presently undertaken to study and to suppress this phenomena in the detector modules.

The carrier dynamics in MCT should enable to increase the bandwidth in MCT APDs to 10 GHz. It has been shown that such a detector can be operated at record high sensitivity levels at ambient temperature which is why the demonstration of such bandwidth is one the key developments for MCT APDs in a near future. At lower already demonstrated bandwidths up to 1 GHz, the aim is to increase the sensitivity to enable single photon detection. This requires to hybridize the APD directly the amplifier to minimize the preamplifier noise and the detector needs to be cooled between 80 and 150 K depending on the BW and required dark count rate.

Finally, we have reported the results of first irradiation ( $10^{11}$  cm<sup>-2</sup> at 180 MeV) and endurance tests at high operating temperature and high reverse bias (-85°C, 12-16 V, 3000 h) on CEA/Leti APDs. These tests have shown that the performance is globally stable. This gives a first indications that CEA/Leti MCT APD technology is well adapted for space application when they are used at high operating temperature and for moderate sensitivity at the order of 10 photons of noise rms. Further tests are required for evaluating the performance at lower operating temperatures required for single photon detection with low DCR.

#### ACKNOWLEDGEMENTS

The authors which to thank CNES, ESA and LABEX FOCUS for supporting this work

#### REFERENCES

- [1] O. Gravrand and J. Rothman, *J. Electron. Mater.*, 40 , 1781 (2011)
- [2] X. Sun; J. B. Abshire; J. D. Beck, *Proc. SPIE*. 9114, 91140K. (2014)
- [3] G. Vojetta, F. Guellec, L. Mathieu, K. Foubert, P. Feautrier, J. Rothman, *Proc. SPIE*, 8375, 83750Y (2012)
- [4] E. de Borniol, J. Rothman, *ICSO*, (2014)
- [5] G. Perrais, J. Rothman, G. Destefanis, J-P. Chamonal, *J. Electron. Mater.*, 37, 1261 (2008)
- [6] G. Perrais, S. Derelle, L. Mollard, J.-P. Chamonal, G. Destefanis, G. Vincent, S. Bernhardt and J. Rothman , *J. Electron. Mater.*, 38, 1790 (2009).
- [7] J. Rothman, et al., *J. Electron. Mater.*, 43, 2947 (2014)
- [8] J. Rothman; E. de Borniol; O. Gravrand; P. Kern; P. Feautrier; J.-B. Le Bouquin; O. Boulade, *Proc. SPIE*. 9915, 99150B. (2016)
- [9] F. Gibert, D. Eduart, C. Cenel, F. Le Mounier, A. Dumas, *Optics Letters*, 40, 3093, (2015)
- [10] D. Tröndle, *et al.*, *Proc. SPIE*, 9739, 973902 (2016)
- [11] J. Rothman, *et. al.*, *Proc. SPIE*, 9647, 96470N (2015)
- [12] I. Zayer, et al., *SpaceOps 2014 Conference*, 1919 (2014).